ISSN 1392-2114 ULTRAGARSAS, Nr.2(28). 1997.

Signal processing for ultrasonic imaging of lossy composites

N.Saffari†, L.Svilainis*

†University College London, UK
**Kaunas University of Technology*

Introduction

Although ultrasonic imaging is popular for visualization of defects within composite materials, its application to certain types of composites produces unsatisfactory results if conventional methods are used. One material for which 'special' techniques have to be developed is high volume-fraction carbon fibre reinforced aluminum matrix composite. This is a very lossy material (with an attenuation of 3.8 dB/mm at 5 MHz). High resolution imaging, which would require using high frequency signals and sharply focused transducers is therefore not possible. If lower frequencies are used, there will be problems with both poor axial and lateral resolutions.

There is also the problem of high structural noise due to scattering from the fibres, even at the lower frequencies. In this paper we report the application of the well-known split-spectrum processing method (SSP) to the anisotropic composite and show that it reduces much of the structural noise. Improvement of the axial resolution is demonstrated using a novel application of Wiener filtering. This technique applied in the conventional sense would be unsatisfactory in the case of this high loss material, because of the difficulty in obtaining a suitable reference 'wavelet'. With proper attenuation compensation and judicious application of Wiener filters to 'split-frequency' signals, we will demonstrate not only an improvement in the axial resolution but also in the structural noise level in images of defects in this composite material.

Experimental set-up

Test specimen is an aluminum-6082 matrix composite with 43% volume fraction of low modulus, long carbon fibre reinforcements in a [0°,90°] lay-up. The thickness of the plate is 12mm. The flat-bottomed holes have three different diameters and are at four different depths from the surface. These holes were used for establishing the performance of the imaging system, before and after signal-processing.

Before the holes were imaged, it was necessary to obtain the attenuation versus frequency characteristic for the specimen. The usual method for measuring attenuation in a plate is to look at the ratio of consecutive backwall echoes. But since the attenuation in this specimen is very high, only one backwall reflection is measurable. Therefore a special through-transmission arrangement was employed which is shown in Fig. 1.

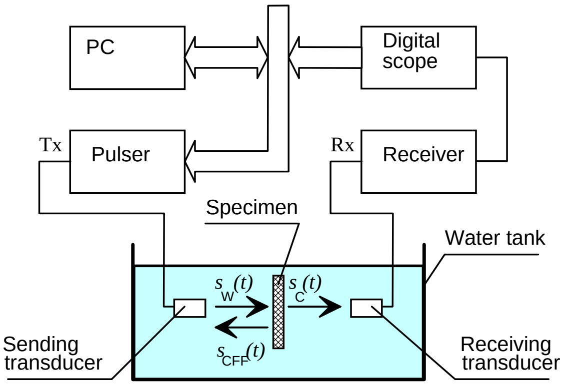

Fig. 1. **Experimental set-up for the attenuation measurement**

In this arrangement three measurements were made with a pair of identical transducers. First the transmitted signal without the composite plate $s_W(t)$ was obtained. Then the composite plate was inserted between the transducers and with the same water path as before, the new transmitted signal $s_C(t)$ and the front face reflection from the plate $s_{CFF}(t)$ were measured. The frequency-dependent attenuation coefficient of the composite is then obtained from the following equation:

$$\alpha_C(f)=\frac{\ln\left[\frac{S_W(f)}{S_C(f)}\left(1-\left(\frac{S_{CFF}(f)}{S_W(f)}\right)^2\right)\right]}{d} \qquad (1)$$

where the signals have been Fourier transformed and *d* is the thickness of the plate. The attenuation coefficient curve is shown in Fig. 2. This curve demonstrates that at a frequency of say 5 MHz the total attenuation in the plate for the backwall echo would be over 90 dBs. The part of curve for frequencies higher than 5MHz looks rather distorted. This is because of high losses in material - it was impossible to obtain reliable measurements here.

The attenuation information was used to choose the best transducer frequency range within which the images were obtained. Bearing in mind that resolution has to be traded-off against lower loss of signal energy, a focused wideband Ultran transducer was chosen with a center frequency of 6MHz and a focal length of 77mm in water.

Complete A-scans were captured for a 64×64 grid over the desired region of the specimen, and the image was then formed by software gating to produce C-scans at chosen depths or B-scan slices. The manner in which the data was collected was different to conventional imaging in the sense that a two-shot operation was employed, where every A-scan is captured at two different gain settings. One gain setting was used to ensure that the front-face echo did not clip, and then a higher gain setting was used to ensure that any smaller reflections from defects were captured at a sufficiently high quantization accuracy. The two traces were then pasted together after the front-face echo, with the correct scaling factor applied. This method was employed as an alternative to time-varying gain compensation, which is sometimes a feature of the more advanced ultrasonic equipment.

The A-scans were collected at a digitization rate of 50MHz with an 8-bit resolution. The traces had 512 sampling points. Most of the processing was subsequently performed on a DEC-Alpha AXP workstation.

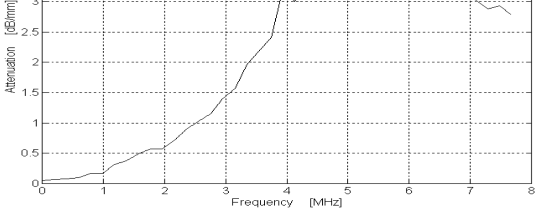

Fig. 2. **Attenuation versus frequency characteristic for the composite sample**

Description of the processing algorithms

The standard signal processing methods were under investigation in order to evaluate whether there is any method available, capable of solving the problems mentioned. Just main algorithms, which performed best or were in later use after corresponding modification are discussed here.

Wiener Filtering

It was thus decided to use a relatively low frequency transducer so that the signal would suffer less attenuation in the specimen. The choice of this transducer which had a long pulse-length produced the first problem in sub-surface imaging of the composite specimen. Low-frequency operation and long pulse-lengths lead to a poor axial (or depth) resolution. Defects that are just below the surface, would have echoes which arrive within the tail of the front-face echo and hence cannot be resolved clearly or at all.

The method commonly used for improving the axial (depth) resolution is Wiener filtering. Implementation of a full Wiener filter requires *a priori* knowledge of the noise spectrum. This is usually not available, so in most practical applications a pseudo-Wiener filter is used which has the following mathematical form:

$$W(f)=\frac{H(f)^*}{\left|H(f)\right|^2+nc} \quad (2)$$

where *H(f)* is the spectrum of the reference wavelet. The noise constant *nc* is used to de-sensitize the filter and ensure that it does not become unstable [1].

Applying this filter to the raw A-scans, *s(t)* leads to a sharpening of the echoes in the time domain, and hence from a long pulse-length signal it should ideally produce a 'spike' if a suitable reference wavelet is used.

The choice of the reference wavelet *h(t)* and the noise constant *nc* is crucial to the correct operation of the Wiener filter. In most applications it is common practice to use the reflection from a polished, flat reflecting surface as the reference wavelet *h(t)*. But here is the first problem with the application of the Wiener filter to the lossy composite in this work: as the acoustic pulse propagates through the composite, attenuation in the sample changes the spectrum of the pulse. The higher frequencies are preferentially attenuated, leading to a shift of the spectrum towards the lower frequency end. So the pulse will have a different frequency characteristic depending on what depth from within the specimen it has been reflected from. The implication of this is that although the reference wavelet, collected as described above, will be well suited to the front face echo, it will not work well for any other reflections from within the specimen. Thus the Wiener filter extracts a spike only for the front face echo.

Another problem is that the noise constant *nc* has to be carefully chosen. The Wiener filter will itself generate spurious ripples that can mask smaller features in the signal. This effect can be reduced by choosing a larger noise constant. A larger noise constant however, will cause a reduction in the depth resolution obtained with the Wiener filter. As shown in [2], possible resolution enhancement depends on the raw data SNR. Once we have large noise presence here, this is the other reason why the Wiener filtering does not perform well.

Split-Spectrum Processing (SSP)

The Split-spectrum processing method has been applied successfully by a number of research groups to enhancement of defect echoes in materials with large grain boundary scattering noise [3,4]. The inhomogeneous nature of the composite specimen used here meant that there was a substantial amount of structural noise present in all signals obtained over the specimen, caused by scattering from the fibres. It was thus decided that the effectiveness of SSP method should be investigated for suppression of this structural noise.

The SSP method starts off by multiplying the broadband signal $s(t)$ spectrum $S(\omega)$ with a number n of identical, equi-spaced Gaussian windows $W_j(\omega)$ that stretch over a relatively high SNR region of the spectrum. The number of such windows depends on the spacing used and the chosen signal bandwidth. Each frequency window is then inverse Fourier transformed to yield a set of time domain 'split' signals. The basic premise of SSP is that all the split signals should contain similar information at those time instants when the defect signal is present. The structural noise however should vary significantly when comparing the split signals. The decision is then established using a nonlinear operation. Several nonlinear operations have been evaluated for processing the split signals. These were averaging, minimization, maximization, quotient of quantiles in order statistical filtering and polarity thresholding [5]. The most effective was found to be maximization followed by polarity thresholding, if the only source of noise is due to the material inhomogeneities. The maximization operation can be described as:

$$s_{\max}(t_i) = \max\left(\left|s_1(t_i)\right|,\ \left|s_2(t_i)\right|, \ldots,\ \left|s_n(t_i)\right|\right) \qquad (3)$$

where $s_j(t_i)$ are the jth frequency window split signals at time instant t_i , n - total number of frequency windows. Polarity thresholding looks for sign reversals among the split signals for each instant in time. If structural noise only is present at a certain time instant, a sign change is expected for some of the split signals. If this happens the output is zeroed for that time instant. If no sign reversal is detected, the maximum value of the split signals at that time instant is used as output.

The new approach

Two improvements are needed to the signal quality, before the B-scan or C-scan image is constructed from the processed A-scans. The first is an SNR enhancement to be achieved by split-spectrum processing (SSP), and the second is a depth resolution enhancement to be obtained by either Wiener filtering.

As explained above, the effectiveness of Wiener filtering depends on the correct choice of the reference wavelet. For high loss materials no suitable reference wavelet can be found, as explained earlier. A new approach is presented here whereby loss compensation is applied to the signals in such a way as to make the use of Wiener filtering more effective, at the same time delivering all the benefits of SNR enhancement obtained with SSP.

The inputs to the process are the reflected signal $s(t_i)$ and a reference wavelet $r(t_i)$ of length m samples. This reference wavelet could be the front face echo from any location on the sample. First both inputs are Fourier transformed to obtain the spectra. Then the same portion of the two spectra is split up by multiplication of each spectrum with the bank of Gaussian windows. The process of 'frequency-selective loss compensation' (FSLC) is applied next. The split frequency windows are inverse Fourier transformed to yield a set of n elements of time domain split signals $sw_j(t_i)$. In Fourier domain it can be written:

$$sw_j(t) = \mathcal{F}^{-1}\left[\mathcal{F}\{s(t)\}\cdot W_j(\omega)\right],\ j = 1,n \qquad (4)$$

here $\mathcal{F}$ and $\mathcal{F}^{-1}$ stands for Fourier transform (forward and back respectively), W_j is Gaussian window:

$$W_j(\omega) = e^{-2\pi\cdot bw\cdot\left(\omega+\omega_j\right)^2} \qquad (5)$$

thus ω_j being the central frequency and bw_j - bandwidth of *j*th window. The same way reference wavelet is split into windows:

$$rw_j(t) = \mathcal{F}^{-1}\left[\mathcal{F}\{r(t)\} \cdot W_j(\omega)\right], j = 1, n \qquad (6)$$

Each split signal is then multiplied by an exponential gain compensation term:

$$sc_j(t_i) = sw_j(t_i) \times e^{a_j \cdot t_i}, i = 1 \ldots m, j = 1 \ldots n \qquad (7)$$

where a_j is the attenuation coefficient at the center frequency of the *j*th Gaussian window; here variable *i* is used to indicate that signals are discrete and that this procedure is performed on each time instance separately. The values used are taken from the experimentally obtained attenuation versus frequency plot for the specimen - see Fig. 2. The reference wavelet is transformed the same way:

$$rc_j(t_i) = rw_j(t_i) \times e^{a_j \cdot t_i}, i = 1 \ldots m, j = 1 \ldots n \qquad (8)$$

Back transformation of the signals to the frequency domain with an FFT completes the compensation process. With both the split signal and the split reference wavelet correctly compensated for the effect of frequency dependent attenuation, a Wiener filter is applied to each split signal before the resulting deconvolved spectrum is transformed again into the time domain.

$$sd(t) = \mathcal{F}^{-1}\left(\mathcal{F}\{sc_j(t)\} \frac{\left[\mathcal{F}\{rc_j(t)\}\right]^*}{\left|\mathcal{F}\{rc_j(t)\}\right|^2 + nc} \right) \qquad (9)$$

This leaves a set of split time domain signals *$sd_j(t)$*, each comprised of a series of narrow spikes. These split signals however still contain both structural noise and any processing noise generated by the Wiener filter. The final stage which is the nonlinear processing of these split signals, performed by either maximization or averaging followed by polarity thresholding, removes most of the structural and filter generated noise. Mathematically polarity thresholding are:

$$\bar{s}_{PT}(t_i) = \begin{cases} \frac{1}{n}\sum_{j=1}^{n} sw_j(t_i), & \left\langle \operatorname{sign}\left(sw_j(t_i)\right) = const \right\rangle \\ 0 & , \left\langle \operatorname{sign}\left(sw_j(t_i)\right) \neq const \right\rangle \end{cases} \qquad (10)$$

$\bar{s}_{pt}$ is an output signal at the time instant t_i.

With the FSLC process, although the exponential time-dependent term in equation (7) amplifies the noise as well as the signal of interest, the subsequent nonlinear processing applied to the split signals effectively removes most of this noise but leaves behind only the amplified signal.

The FSLC process is expected to make the performance of the Wiener filter less sensitive to the choice of the reference wavelet. This should enable one to use the front face echo as the reference *r(t)* and still obtain a sharpening of a deep defect echo. If the signal spectrum is split into narrow enough windows, it is even possible to use a Gaussian reference wavelet without losing any detail from the Wiener filtered signal, but in that case resolution enhancement is much less.

Results and discussion

The following examples serve to demonstrate the improvements in the SNR and resolution obtained with the processes described above.

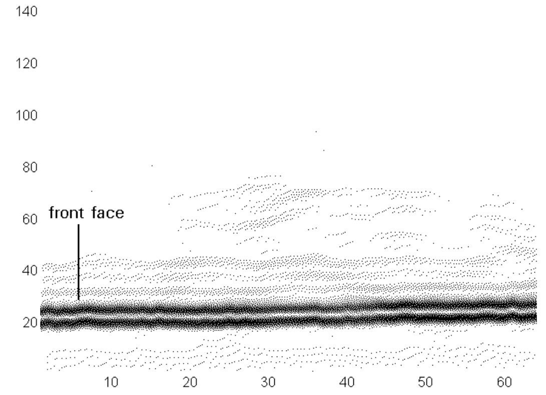

Fig. 3. **The unprocessed B-scan of the specimen sliced through a hole 2mm below surface.**

Fig. 3 is a raw, unprocessed B-scan of the specimen, sliced through a 10mm diameter hole, 2mm below the surface. It is apparent that apart from a large front face echo, nothing is visible below the surface. If the gain is increased such that the front face echo is now clipped, as seen in the A-scan of Fig. 4 (top), the long ringing of the front face echo and the structural noise become more apparent. Fig. 4 (bottom) shows the result of processing the same signal according to the new scheme [6]. Here frequency-selective loss compensation and Wiener filtering have been incorporated within SSP as per new scheme. The remarkable improvement in SNR and the sharpening of the hole echo is evident.

Fig. 5 and Fig. 6 show B-scans for when Wiener filtering only and SSP only is applied in the conventional manner. These show that although Wiener filtering is commonly used for resolution enhancement, it fails to pick out the hole echo. What is constructed is a sharp spike for the

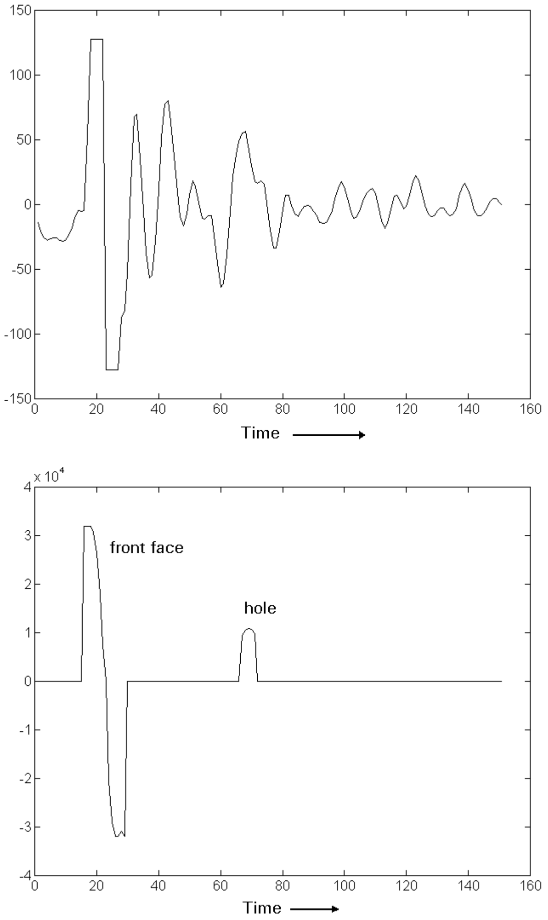

Fig. 4. **A-scans of unprocessed (top) and processed (bottom) signals.**

front face echo together with substantial noise generated by the filtering process. Any signal from the hole is masked by this process noise.

With SSP only, one would expect an SNR improvement. This can indeed be seen in Fig. 6 where the hole echo is also evident. Some structural noise is left behind and the front face echo is much wider than in figure Fig. 5 as expected. The hole image is however not complete as some of the information seems to have been lost in the process. Fig. 6 shows the B-scan for the same hole when the new approach is used.

As in the A-scan of Fig. 4 (bottom), FSLC and Wiener filtering have been incorporated into SSP, and a Gaussian reference wavelet has been used. This image is a much more acceptable reconstruction of the hole, which is now clearly resolved, correctly sized (with some lateral spread) and with a very high SNR everywhere in the image.

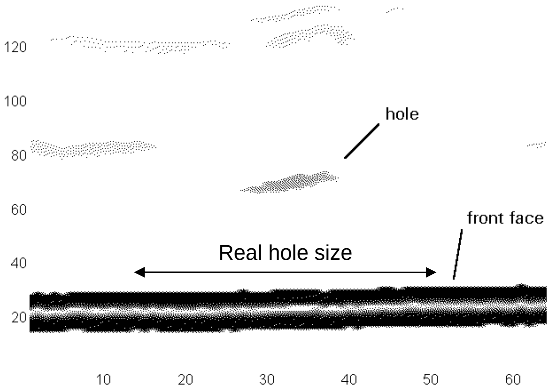

Fig. 6. **Result of Split-spectrum processing only.**

In order to make additional prove for FSLC performance, results check-up, using X-ray radiography and computed tomography was done. Sample was exposed for additional radiography investigation. The investigation was dedicated to check for additional feature, extracted in front of hole at Fig.7. Closer investigation of X-ray radiography revealed that the fibres structure was distorted exactly on the hole which was examined by FSLC and exposed the natural defect.

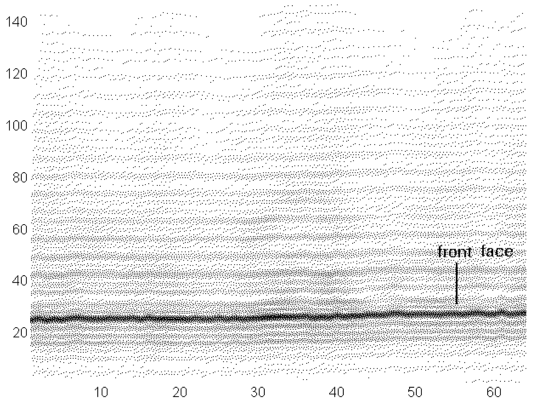

Fig. 5. **Result of Wiener filtering only.**

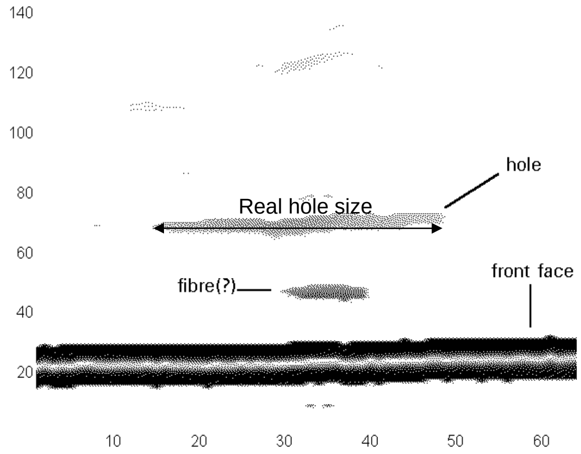

Fig.7. **Result of application of the new processing method.**

Fig. 8 is showing zoomed part of X-ray image. The image was computer preprocessed is order to improve the visibility of details. It seems that during aluminum extrusion into carbon matrix, structure was destroyed here. This gave a large variations in density, which is seen at X-radiograph, and gave additional reflection after FSLC processing.

Conclusions

A new signal processing scheme has been proposed for ultrasonic imaging of high loss composite structures. The new scheme incorporates a frequency-selective loss compensation and Wiener filtering within a split-spectrum processing algorithm. This approach greatly enhances the signal-to-noise ratio and improves the depth resolution for images obtained in a specimen of high acoustic noise level.

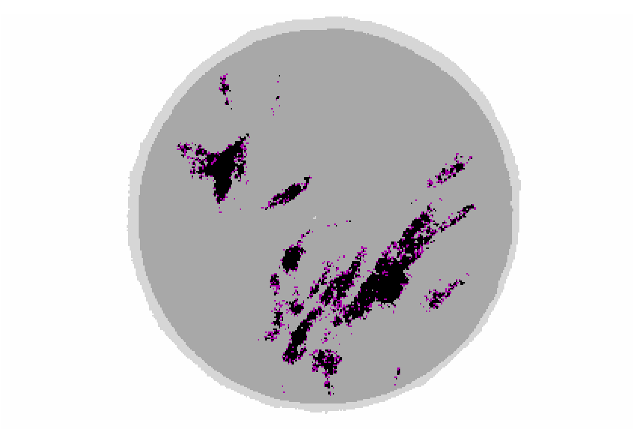

Fig. 8. **Zoomed area of X-radiograph, presenting examined hole.**

In comparison with other signal processing methods it shoved the best performance. It could be applied to wider range of composites, not just for carbon fibre reinforced aluminum matrix composite. The good performance of the algorithm can be explained by time-frequency dependent signal components proper correction by FSLC, which then contributes to good SSP algorithm performance and excellent interaction of Wiener and SSP properties. The X-ray radiography confirmed the results obtained by ultrasound.

Acknowledgments

We are grateful to our friends from Linköping University, Sweden for their help in producing X-rays radiography images.

References

1. **R.C. Gonzalez and R.E. Woods** Digital Image Processing, Addison-Wesley (1992).
2. **V.Sukhorukov, E.Vainberg, R.Kazys** Non-destructive testing. Imaging and automation of testing Vol 5 (Vysshaja shkola) Moscow (1993) Ch 5 (in Russian)
3. **K.D. Donohue. J. M. Bressler, T.Varghese, and N. M. Bilgutay** Spectral correlation in ultrasonic pulse-echo signal processing, IEEE Transactions on Ultrasonics Ferroelectrics and Frequency Control, Vol-40, (1993), pp 330-337.
4. **V.L.Newhouse, Guo Yao Li, Yue Li** A split spectrum processing method of scaterer density estimation, NATO ASI series, (1988), Vol. F44
5. **J. Saniie, D.T. Nagle and K.D. Donohue** IEEE Trans. on Ultrasonics, Ferroelectrics and Freq. Control, Vol 38(2), (1991), pp. 133-140.
6. **L.Svilainis, N.Saffari, H.Mahlouji**. Signal processing for ultrasonic imaging of composites. Conference proceedings. Bentham Press, London. (1994) p.p.138-153

N.Saffari, L.Svilainis

Signalø apdorojimas atliekant smarkiai slopinanèiø kompozitiniø medþiagø ultragarsinæ vizualizacijà

Reziume

Sukurtasis aukðtu struktûriniø triukðmø lygiu pasiþyminèiø kompozitiniø medþiagø tyrimo metodas leidþia sumaþinti struktûriniø triukðmø lygá bei padidinti skiriamumà tiriant nehomogenines medþiagas. Naujuoju signalo apdorojimo metodu gaunami daug geresni rezultatai nei kitais metodais.

DOI: 10.5755/j01.u.28.2.7861